Energy 77 (2014) 305–317

Contents lists available at ScienceDirect

Energy

journal homepage: www.elsevier.com/locate/energy

Multi-objective thermal analysis of a thermoelectric device: Influence of geometric features on device characteristics

Amin Ibrahim [a, *], Shahryar Rahnamayan [a], Miguel Vargas Martin [a], Bekir Yilbas [b]

[a] University of Ontario Institute of Technology, Faculty of Engineering and Applied Science, 2000 Simcoe Street North, Oshawa, Ontario L1H 7K4, Canada
[b] Mechanical Engineering Department, King Fahd University of Petroleum and Minerals, Dhahran, Saudi Arabia

ARTICLE INFO

Article history:
Received 10 November 2013
Received in revised form
7 August 2014
Accepted 9 August 2014
Available online 3 October 2014

Keywords:
Thermoelectric generator
Efficiency
Output power
NSGA-II (non-dominated sorting genetic algorithm-II)
GDE3 (generalized differential evolution generation 3)
SMPSO (speed-constrained multi-objective particle SWARM OPTIMIZATION)

ABSTRACT

Proper assessment of geometric features of a thermoelectric generator is important to design devices with improved performance features such as high efficiency and output power. In the present study, three the-state-of-the-art multi-objective evolutionary algorithms, namely, NSGA-II (Non-dominated Sorting Genetic Algorithm-II), GDE3 (Generalized Differential Evolution generation 3), and SMPSO (Speed-constrained Multi-objective Particle Swarm Optimization) are used to optimize the geometric features of a thermoelectric generator for improved efficiency and output power while incorporating different operating conditions. The parameters assessing geometric features of the device include shape factor and pin length size while operating parameters include temperature ratio and external load parameter. Thermal analysis incorporating geometric features and operating parameters of the device is introduced prior to the optimization study. The findings are validated against the results reported in the open literature. It is found that shape factor and pin length size have significant effect on the device performance. Increasing shape factor ($S \leq 0.5$) first increases thermal efficiency to reach its maximum (~17%), and furthermore, an increase in shape factor ($S \geq 0.5$) lowers thermal efficiency significantly (~8%). Device output power behaves similar to that of efficiency for small increment in shape factor, provided that further increase in shape factor does not influence output power of the device. A unique design configuration is present for a fixed operating condition of a thermoelectric generator; in which case, thermal efficiency and output power of the device attain high values.

1. Introduction

Increasing demand for electrical energy consumption led to the development of efficient energy conversion devices, which use clean energy resources. Sustainable development of energy efficient devices requires extensive research into design and operation of the electrical energy generation devices through integration of renewable energy technologies. Thermoelectric power generator is one of these devices, which involves efficient electrical energy generation from waste heat. Although efficiency of traditional thermal to electric generators is several times higher than the efficiency of a thermoelectric system for large electrical power generation applications, the traditional systems are expensive, due to large scale energy requirements, and they operate at high temperatures. On the other hand, for applications requiring less than 100 W, thermoelectric generators become less costly and have several advantages over the traditional thermal to electric generators [1]. The recent developments in thermoelectric materials extend the thermodynamics analysis to cover high temperature ranges. This is vital since the efficiency of a thermoelectric converter depends heavily on the temperature differences. In addition, efficiency of thermoelectric devices can also be enhanced through modifying device geometric configurations [2–4]. Consequently, investigation into influence of geometric configuration of thermoelectric generator on device performance including efficiency and power becomes essential.

Considerable research studies have been carried out to examine thermoelectric device performance for various applications. Exergy analysis and performance assessment of thermoelectric generator were carried out by Wang et al. [5]. Their findings revealed that both the maximum energy efficiency and exergy efficiency increased with increasing hot-reservoir temperature for the case where the Seebeck coefficient and thermal conductivity was temperature-dependent. Performance of a solar heat pipe

* Corresponding author. 2000 Simcoe Street North (UB-3020), Oshawa, Ontario L1H 7K4, Canada. Tel.: +1 905 721 8668x5355.
E-mail addresses: Amin.Ibrahim@uoit.ca, amin.ibrahim@gmail.com (A. Ibrahim), Shahryar.Rahnamayan@uoit.ca (S. Rahnamayan), Miguel.VargasMartin@uoit.ca (M. Vargas Martin), bsyilbas@kfupm.edu.sa (B. Yilbas).

http://dx.doi.org/10.1016/j.energy.2014.08.041
0360-5442/

thermoelectric generator unit was carried out by He et al. [6]. They presented the influence of basic parameters on device performance. These parameters included solar irradiation, cooling water temperature, thermo-element length and cross-section area, and a number of thermo-elements. Efficiency improvement of thermoelectric generators was investigated by Patyk [7]. He demonstrated that, under various operating conditions, thermoelectric generators in power units could save waste energy and reduce the environmental burden due to their eco-efficient characteristics. Parametric and exergetic analysis of waste heat recovery system based on thermoelectric generator was carried out by Shu et al. [8]. They suggested that combined thermoelectric and an organic cycle system was suitable for waste heat recovery from engines. In this case, thermoelectric generation could extend the temperature range of a heat source and thereby improve the fuel economy of engines.

Thermoelectric energy conversion incorporating linear and nonlinear temperature dependence of material properties was examined by Wee et al. [9]. They indicated that inclusion of the Thomson effect was essential to assess the qualitative behavior of thermoelectric energy conversion system. Influences of effective temperature differences and electrical parameters on performance of thermoelectric generators were studied by Kim [10]. He showed that approximately 25% of the maximum output power was lost because of the parasitic thermal resistance of the thermoelectric module. Efficiency analysis of thermoelectric combined energy systems was carried out by Chen et al. [11]. They indicated that the overall conversion efficiency of the thermal system could be improved significantly through integration of thermoelectric devices.

With regard to multi-objective optimization, a few notable recent studies have been carried out to investigate the performance of thermoelectric devices under various operating conditions and device configurations. Rao and Patel [12] successfully utilized a modified TLBO (Teaching-Learning based multi-objective optimization) algorithm to maximize the cooling capacity and the coefficient of performance of TEC (thermoelectric cooler). In this study they have considered two different configurations of TECs, electrically separated and electrically connected in series as well as the contact and spreading resistance of the TEC. On the other hand Belanger and Gosselin [13] developed a simulation model of a heat exchanger with thermoelectric generators in its walls to optimize the total volume, total number of thermoelectric modules, output power, and pumping power. Their results showed that the number of sub-channels in the heat exchanger has a more significant impact on the overall performance than the fin geometry. Moreover, the net output power is largely dependent on the number of thermoelectric modules but not on the heat exchanger volume. NSGA-II was widely used in optimization of thermal systems for improved performances [14–23]. Optimization of thermodynamic system incorporating an ammonia-water power cycle was carried out by Wang et al. [14]. They demonstrated that the optimization provided the useful information to maximize the exergy efficiency and minimize the total heat transfer capability and turbine size parameter under the given waste heat conditions. The Pareto optimal solutions for an Organic Rankine Cycle for diesel engine waste heat recovery system were introduced by Hajabdollahi et al. [15] using the NSGA-II algorithm. They indicated that the algorithm used maximized the thermal efficiency and minimized the total annual cost simultaneously. Design and optimization of a tubular recuperative heat exchanger used in a regenerative gas turbine cycle were carried out by Sayyaadi et al. [16]. They showed that the multi-objective optimization scenario incorporating the NSGA-II algorithm could be considered as a generalized optimization approach in which balances between economical viewpoints of both heat exchanger manufacturer and end user of recuperater could be achieved. Systematic analysis of the heat exchanger arrangement problem using multi-objective genetic optimization was presented by Daroczy et al. [17]. In the analysis, they considered the conditions, which were particularly suited for low-power applications, as found in a growing number of practical systems in an effort toward increasing energy efficiency.

Recently, Ibrahim et al. [18] have used the NSGA-II and GDE3 algorithms to investigate the optimal PV (photovoltaic) farm design yielding the maximum field incident energy collected while minimizing the deployment cost of PVs in the Toronto area, Canada. They were able to find a diverse set of optimal PV farm design solutions which would not be possible to achieve similar result using single objective algorithms.

With regard to energy planning, Silva et al. [35] have utilized three recent PSO (Particle Swarm Optimization) based multi-objective optimizers, MOPSO-CDR, MOPSO-DFR, and SMPSO to investigate the optimal operational planning involving hydrothermal systems composed of eight Brazilian hydroelectric plants. The optimization problem involved minimizing the total cost of thermal power while maximizing the total stored energy in all reservoirs. They have shown that it is possible to approach the planning of hydrothermal systems as a multi-objective problem.

The performance characteristics of thermoelectric devices, mainly, depend on the design parameters and operating conditions. The design configuration can be improved through the enhancement of the average Figure of Merit ($ZT_{average}$) and re-sizing of the thermoelectric active elements such as thermoelectric pins [2]. Enhancement of the averaged Figure of Merit requires improvement in the pin materials, such as Bi_2Te_3 and Skutterudites [24]. Since the improvement of the device active material involves material science research, this is not considered in the present study. However, the influence of geometric configurations on thermal performance of thermoelectric devices was investigated previously [2–4], where the main focus was the assessment of device performance as a result of a single parametric variation. Therefore, the geometric parameters maximizing device performance are considered in the present study in line with the previous findings [2–4]. However, optimization study for device performance considering all geometric configurations under various operating conditions was not thoroughly investigated. Moreover, the two objectives, namely, the maximization of power and efficiency are conflicting objectives. To fill out this gap, the present study uses three state-of-the-art multi-objective evolutionary algorithms, namely, NSGA-II, GDE3, and SMPSO to optimize the efficiency and the output power of a thermoelectric device. The optimization of thermoelectric device performance due to different device geometric configurations and operating conditions are presented, yielding an analysis of optimum device geometric configurations for high thermal efficiency and output power.

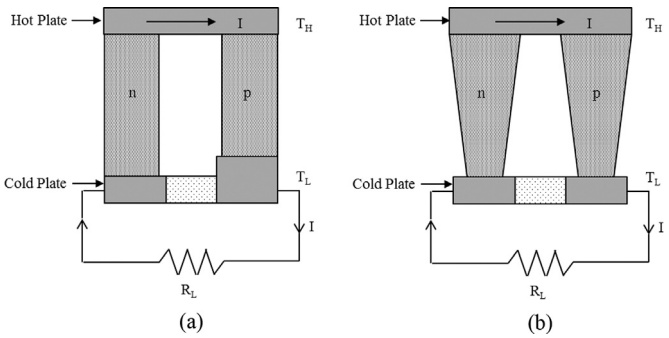

Fig. 1. A schematic view of thermoelectric generator for different geometric configurations: a) size of pin legs is different and b) shape factor is different.

2. Analysis of a thermoelectric device

2.1. Thermal analysis

Thermal efficiency of the thermoelectric generator due to pin geometric configurations, as shown in Fig. 1, can be written as [3]:

$$\eta = \frac{I^2 R_L}{\alpha I T_1 + K(T_1 - T_2) - \frac{1}{2} I^2 R}, \tag{1}$$

where K is the thermal conductance and R is the electrical resistivity of the thermoelectric generator.

The current I is a function of the net Seebeck coefficient $\alpha = \alpha_p - \alpha_n$ (the difference between the Seebeck coefficients of p and n junctions), the upper and lower junction temperatures (T_1 and T_2), the electrical resistance R and the external load resistance R_L as:

$$I = \frac{\alpha(T_1 - T_2)}{R_L + R}. \tag{2}$$

Substituting Equation (2) in Equation (1) the efficiency becomes

$$\eta = \frac{\alpha^2 (T_1 - T_2) R_L}{K(R_L + R)^2 + \alpha^2 T_1 (R_L + R) - \frac{1}{2}\alpha^2 (T_1 - T_2) R}. \tag{3}$$

The cross-sectional area of the pin (leg) of the thermoelectric generator, as shown in Fig. 2, can be written as [3]:

$$A(x) = A_0 + S\left(x - \frac{L}{2}\right)\delta, \tag{4}$$

where A_0 is the average (mid-height) cross-sectional area, L is the height of the pin, δ is the thickness of the pin, and S is the shape factor of the pin, i.e.,

$$S = \frac{1}{\delta}\frac{\mathrm{d}A}{\mathrm{d}x}. \tag{5}$$

The heat transfer rate through the leg along x is given by

$$\dot{Q} = -kA(x)\frac{\mathrm{d}T}{\mathrm{d}x} \tag{6}$$

After assuming a steady heating situation and isolated leg surfaces, the rate of heat transfer along the x-axis in the pin can be written as [3]:

$$\dot{Q} = \frac{kS\delta}{\ln\left(\frac{A_0 + S\delta\frac{L}{2}}{A_0 - S\delta\frac{L}{2}}\right)}(T_1 - T_2). \tag{7}$$

The overall thermal conductance of the pin in Equation (7) is:

$$K_{\mathrm{leg}} = \frac{kS\delta}{\ln\left(\frac{A_0 + S\delta\frac{L}{2}}{A_0 - S\delta\frac{L}{2}}\right)}. \tag{8}$$

Total thermal conductance of the thermoelectric generator due to two pins can be written as:

$$K = \frac{(k_p + k_n)S\delta}{\ln\left(\frac{A_0 + S\delta\frac{L}{2}}{A_0 - S\delta\frac{L}{2}}\right)}, \tag{9}$$

where k_p and k_n are the thermal conductivities of the p-type and n-type pins, respectively.

The overall electrical resistance of the pin ($R_{\mathrm{leg}} = \int_0^L (\mathrm{d}x/kA(x))$) can be obtained by substituting $A(x)$ from Equation (5) and performing the integration; therefore, the overall electrical resistance becomes:

$$R_{\mathrm{leg}} = \frac{1}{k_e m \delta}\ln\left(\frac{A_0 + S\delta\frac{L}{2}}{A_0 - S\delta\frac{L}{2}}\right). \tag{10}$$

Thus, the total electrical resistance of the thermoelectric generator due to two pins is given by:

$$R = \left(\frac{1}{k_{e,p}} + \frac{1}{k_{e,n}}\right)\frac{1}{S\delta}\ln\left(\frac{A_0 + S\delta\frac{L}{2}}{A_0 - S\delta\frac{L}{2}}\right) = \frac{k_{e,p} + k_{e,n}}{k_{e,p}k_{e,n}S\delta}\ln\left(\frac{A_0 + S\delta\frac{L}{2}}{A_0 - S\delta\frac{L}{2}}\right), \tag{11}$$

where $k_{e,p}$ and $k_{e,n}$ are the electrical conductivities of the p-type and n-type pins, respectively.

Substituting Equations (9) and (11) in Equation (3), efficiency of the thermoelectric generator can be written in dimensionless form as [3]:

$$\eta = (1-\theta)\frac{2ZT_{\mathrm{ave}}\left(1 + \sqrt{\frac{r_k}{r_{\mathrm{ke}}}}\right)^2\left(\frac{R_L}{R_0}\right)}{(1+\theta)\left(\frac{K}{K_0}\right)\left(\frac{R_L}{R_0} + \frac{R}{R_0}\right)^2 + 2ZT_{\mathrm{ave}}\left(1 + \sqrt{\frac{r_k}{r_{\mathrm{ke}}}}\right)^2\left[\frac{R_L}{R_0} + \frac{1}{2}\frac{R}{R_0}(1+\theta)\right]}, \tag{12}$$

where $\theta = T_2/T_1$ is the temperature ratio; $r_k = k_p/k_n$ is the thermal conductivity ratio; $r_{ke} = k_{e,p}/k_{e,n}$ is the electrical conductivity ratio; $ZT_{\mathrm{ave}} = ((\alpha^2(k_{e,n}/k_n)T_1)/(1 + \sqrt{r_k/r_{\mathrm{ke}}})^2)(1 + \theta/2)$ is the figure of merit based on the average temperature; $K_0 = A_0 k_n/L$ is the reference thermal conductance; and $R_0 = L/A_0 k_{e,n}$ is the reference electrical resistivity of the thermoelectric device.

Hence, the overall thermal conductance and overall electrical resistivity can be written in dimensionless form as:

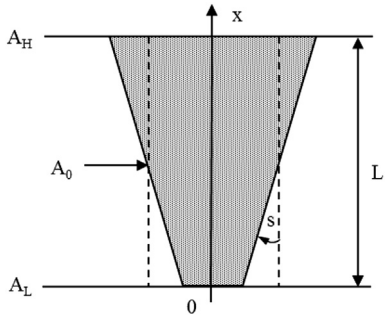

Fig. 2. Schematic view of geometric configuration of thermoelectric pin.

$$\frac{K}{K_0} = \frac{\mu(r_k+1)}{\ln\left(\frac{1+\mu/2}{1-\mu/2}\right)} \tag{13}$$

and

$$\frac{R}{R_0} = \left(\frac{1+r_{ke}}{r_{ke}}\right)\frac{\ln\left(\frac{1+\mu/2}{1-\mu/2}\right)}{\mu}, \tag{14}$$

where μ is the dimensionless slope parameter and is defined as $\mu = S\delta L/A_0$.

The power generation from the thermoelectric power generator is $\dot{W} = I^2R_L$, which yields:

$$\dot{W} = \frac{\alpha^2(T_1-T_2)^2}{(R_L+R)^2}R_L. \tag{15}$$

And thus the dimensionless power generation can be written as [3]:

$$\frac{\dot{W}}{K_0T_2} = 2\frac{(1-\theta)^2}{\theta(1+\theta)}\frac{ZT_{ave}\left(1+\sqrt{\frac{r_k}{r_{ke}}}\right)^2\left(\frac{R_L}{R_0}\right)}{\left(\frac{R_L}{R_0}+\frac{R}{R_0}\right)^2}. \tag{16}$$

2.2. Optimization of thermoelectric device for the maximum efficiency and output

Multi-objective optimization is the process of simultaneously optimizing two or more conflicting objective functions subject to several certain constraints. A multi-objective optimization problem can be defined as:

$$\begin{aligned} \text{Min/Max}: \quad & F(x) = [F_1(x), F_2(x), \ldots, F_m(x)] \\ \text{Subject to}: \quad & G(x) = [G_1(x), G_2(x), \ldots, G_n(x)] \geq 0 \\ & H(x) = [H_1(x), H_2(x), \ldots, H_j(x)] = 0 \\ & x_i^L \leq x_i \leq x_i^L, i = 1, \ldots, k \end{aligned} \tag{17}$$

where m ($m \geq 2$) is the number of objectives; $x = (x_1,\ldots,x_k)$ is the vector representing the decision variables, F represents the vector of objectives to be optimized, G represents the set of feasible solutions associated with inequality constraints, H represents the set of feasible solutions associated with equality constraints, and $[x_i^L, x_i^L]$ are the lower and upper bound for each decision variable x_i.

A large number of metaheuristics were successfully utilized to solve real-life problems, including MOP (multi-objective problems). Since 1960 there have been major developments in the metaheuristics field [25].

The optimal solution for MOPs is not a single solution as for mono-objective problems, so a set of solutions defined as Pareto optimal solutions. A solution is Pareto optimal if it is not possible to improve a given objective without deteriorating at least another objective. The main goal of the resolution of a multi-objective problem is to obtain the Pareto optimal set and, consequently, non-dominated solutions known as the Pareto front.

An objective vector $u = (u_1,\ldots,u_n)$ is said to dominate another vector $v = (v_1,\ldots,v_n)$ (denoted by $u \prec v$) if and only if no component of v is smaller than the corresponding component of u and at least one component of u is strictly smaller, assuming a minimization problem. That is,

$$\forall i \in \{1,\ldots,n\} : u_i \leq v_i \wedge \exists\, j \in \{1,\ldots,n\} : u_j < v_j. \tag{18}$$

The current optimization problem is composed of two problems: the optimization of the output power and efficiency of a thermoelectric device without considering the shape factor (see Fig. 1(a)) and the optimization of the output power and efficiency of a thermoelectric device when considering the shape factor (see Figs. 1(b) and 2). The optimization problem without the shape factor comprises of two objectives and seven variables; while the optimization problem with the shape factor contains two objectives and six variables. These two objectives in both problems are the maximization of thermal efficiency (η) and output power ($\dot{W}$) based on Equations (1) and (15), respectively. The seven variables used in the first problem are the upper and lower temperatures (T_1 and T_2), the external load resistance (R_L), the cross-sectional area of the pins (A_n and A_p), and the height of the pins (L_n and L_p). The six variables used in optimization with shape factor are the same as the above-mentioned variables except A_n and A_p are replaced by the average (mid-height) cross-sectional area of the pin (A_o), L_n and L_p replaced by the average pin height (L) and additional variable, the shape factor (S). The mathematical formulation of the optimization problem is defined as follows:

Maximize (For both optimization problems):

$$\eta = \frac{I^2R_L}{\alpha IT_1 + K(T_1-T_2) - \frac{1}{2}I^2R}$$

$$\dot{W} = \frac{\alpha^2(T_1-T_2)^2}{(R_L+R)^2}R_L$$

Variable Bounds (Optimization without Shape Factor):

The upper and lower junction temperatures range between 273 K (0°C) and 600 K (327°C).

$$300 \leq T_1 \leq 600 \tag{19}$$

$$273 \leq T_2 \leq 400 \tag{20}$$

The external load resistance is kept at a maximum of 100Ω.

$$0.1 \leq R_L \leq 100 \tag{20a}$$

The cross-sectional area of the pins and the height the pins capped to:

$$10^{-6} \leq A_n \leq 5.0\times10^{-4}\left(\mathrm{m}^2\right) \tag{21}$$

$$10^{-6} \leq A_p \leq 5.0\times10^{-4}\left(\mathrm{m}^2\right) \tag{22}$$

$$10^{-3} \leq L_n \leq 4.0\times10^{-3}(\mathrm{m}) \tag{23}$$

$$10^{-3} \leq L_p \leq 4.0\times10^{-3}(\mathrm{m}) \tag{24}$$

Variable Bounds (Optimization with Shape Factor):

$$300 \leq T_1 \leq 600 \tag{25}$$

$$273 \leq T_2 \leq 400 \tag{26}$$

$$0.1 \leq R_L \leq 100 \tag{27}$$

$$10^{-6} \leq A_o \leq 5.0\times10^{-4}\left(\mathrm{m}^2\right) \tag{28}$$

$$10^{-3} \leq L \leq 4.0\times10^{-3}\left(\mathrm{m}\right) \tag{29}$$

The shape factor is limited between 0 and 1. The zero shape factors correspond to vertically parallel pins while 1 corresponds to a horizontal pin (this is an extreme case implying the contact area of the lower junction is 0). The shape factor 0.5 corresponds to pin vertical slope of 45°.

$$0 \leq S < 1 \tag{30}$$

where:

$T_1, T_2, R_L, A_n, A_p, A_0, L_n, L_p, L \in \mathbb{R}$.

As previously stated, in the current study we utilized three state-of-the-art multi-objective algorithms, namely, NSGA-II, GDE3 and SMPSO. NSGA-II is a very popular evolutionary multi-objective algorithm that has been successfully utilized in many real-life optimization problems. GDE3 is an extension of one of the most successfully adopted single-objective algorithm called DE. GDE3 has shown comparable performance to many of the state-of-the-art multi-objective algorithms in numerical problems [31,32]. SMPSO is a recent adaption of the PSO algorithm and it has shown favorable results among numerous PSO based multi-objective algorithms.

2.2.1. NSGA-II

The NSGA-II (non-dominated sorting genetic algorithm II) algorithm is a popular fast elitist multi-objective, non-domination based genetic algorithm [26]. It is able to find well-spread solutions over the Pareto-optimal front and requires a low computational complexity $O(mN^2)$; where m is the number of objectives and N is the population size. The main components of NSGA-II are elite-preserving operator (preserving and using previously found best solutions in subsequent generations), non-dominated sorting (sorting population into a hierarchy of sub-populations based on the ordering of Pareto dominance) and crowded tournament selection operator to preserve the diversity among non-dominated solutions in the later stage of the run in order to obtain a good spread of solutions. The NSGA-II algorithm and parameter settings used in all our experiments are presented in Algorithm 1 and Table 1, respectively.

Table 1
Parameters' settings used in all experiments and L is the individual length.

NSGA-II parameters' setting [26]	
Population size	100
Initial population	Uniform random
Maximum function evaluation	10^6
Mutation probability	$1.0/L$
Crossover probability	0.9
Mutation distribution index	20
Crossover distribution index	20
Number of runs	100
GDE3 parameters' setting [33]	
Population size	100
Initial population	Uniform random
Maximum function evaluation	10^6
Mutation probability	0.5
Crossover probability	0.9
Number of runs	100
SMPSO parameters' setting [30]	
Swarm size	100
Initial swarm	Uniform random
Maximum function evaluation	10^6
Mutation probability	$1.0/L$
Archive size	100
Number of runs	100

2.2.2. GDE3

GDE3 (Generalized Differential Evolution generation 3) is an extension of DE (Differential Evolution) for global optimization with an arbitrary number of objectives and constraints [33]. GDE3 with a single objective and without constraints is similar to the original DE. GDE3 improves earlier GDE versions in the case of multi-objective problems by giving better distributed solutions. GDE3 modifies earlier GDE versions using a growing population and non-dominated sorting with pruning of non-dominated solutions to decrease the population size at the end of each generation. This improves the obtained diversity and makes the method more stable for the selection of control parameter values. The GDE3 algorithm and parameter settings used in all our experiments are shown in Algorithm 2 and in Table 1, respectively.

Algorithm 1: NSGA-II Algorithm

```
Generate initial population (uniform randomly);
Evaluate objective values
Assign rank (level) based on Pareto dominance
Generate child population
    Tournament selection
    Recombination and mutation
for i = 1 to number of generations do
    for all Parent and child population do
        Assign rank based on Pareto
        Generate sets of non-dominated fronts
        Determine the crowding distance among
        points on each front
    end for
    Select elitist points based on rank and crowding
    distance
    Create next generation
        Tournament Selection
        Recombination and Mutation
end for
```

Algorithm 2: GDE3 Algorithm

Generate uniform random parent population of NP individuals.
Set $m = 0$
Evaluate objective values
for $i = 1$ to number of generations **do**
  for all Parent population **do**
    Evaluate objective values for the trial vector
    Selection process:

$$x_i, G+1 = \begin{cases} u_i, G+1, & if\ u_i, G+1 \preccurlyeq x_i, G \\ x_i, G & otherwise \end{cases}$$

    Set $m = m+1, x_{NP+m}, G+1 = u_i, G+1$
    If $\forall j: gj(u_i, G+1) \leq 0 \wedge x_i, G+1 == x_i, G+1 \wedge u_i, G \preccurlyeq u_i, G+1$
  end for
  Create next generation
  Apply non-dominated ranking to $NP + m$ vectors. Select NP non-dominated vectors and set $m = 0$.
end for

2.2.3. SMPSO

SMPSO (Speed-constrained Multi-objective PSO) is an extension of PSO (particle swarm optimization) [30]. PSO simulate the behavior of a flock of birds. In PSO, each solution is a “particle” and each particle has two values: fitness value which is calculated by the fitness function, and velocity which indicates the direction of particles [34]. There are mainly three differences between SMPSO and PSO: SMPSO incorporates a velocity constriction mechanism to limit the maximum velocity of the particles; it uses polynomial mutation as a turbulence factor; and it has an external archive to store the non-dominated solutions found during the search. The

SMPSO algorithm and parameter settings used in all our experiments are shown in Algorithm 3 and in Table 1, respectively.

Algorithm 3: SMPSO Algorithm

```
Initialize Swarm //uniform random
Evaluate swarm
Initialize leaders archive
Generation = 0
for i = 1 to number of generations do
    Compute speed //Using constriction mechanism
    Update position
    Mutation //Turbulence
    Evaluate swarm
    Update leaders archive
    Update particle memory
end for
```

3. Results and discussion

Optimization study of thermoelectric power generator for improved thermal efficiency and output power is considered, and the optimum device geometric configuration is identified. Thermal efficiency and output power are formulated in terms of device geometric configurations. The findings are validated against the results of previous studies [3,4]. The parameters incorporated in the two optimization problems include shape factor, length of the pins, external load parameter, and operating temperature ratio. It should be noted that shape factor and pin length size define the geometric features of the device while external load parameter and operating temperature ratio are related to the operating conditions of the device.

Due to the stochastic nature of heuristic algorithms, the proposed algorithms were executed 100 times and the stopping criterion was set to 10^6 function evaluations. In addition, the HV (hyper-volume) measure [27] was used to compare the performance of each result. The HV indicator is a very popular and widely used measure of fitness of Pareto set [27]. This indicator measures the volume of the dominated portion of the objective space. The interest in this indicator stems from the fact that it contains the strict Pareto compliance which is a highly desirable feature. In other words HV takes into consideration both the accuracy of a solution set and the diversity of a solution set.

The HV is obtained by computing the volume of the non-dominated set of solutions Q for minimization multi-objective optimization problems. For every solution Q, a hypercube v_i is generated with a reference point W and the solution i as its diagonal corner. The reference point W can be generated by building a vector of worst possible objective function values. Then, the HV is computed as a union of all the found hypercubes as follows:

$$\mathrm{HV} = \mathrm{volume}\left(\bigcup_{i=1}^{|Q|} v_i\right) \tag{31}$$

3.1. Optimization without the shape factor

In order to validate the optimization results, we have conducted the first optimization problem to determine the influence of operating and device parameters of the thermoelectric device on the maximum efficiency and the maximum output power (see Fig. 1(a)). Figs. 3(a), 4(a) and 5(b) present the distribution of Pareto-optimal solutions (based on the best HV results) obtained by the proposed algorithms, NSGA-II, GDE3 and SMPSO respectively.

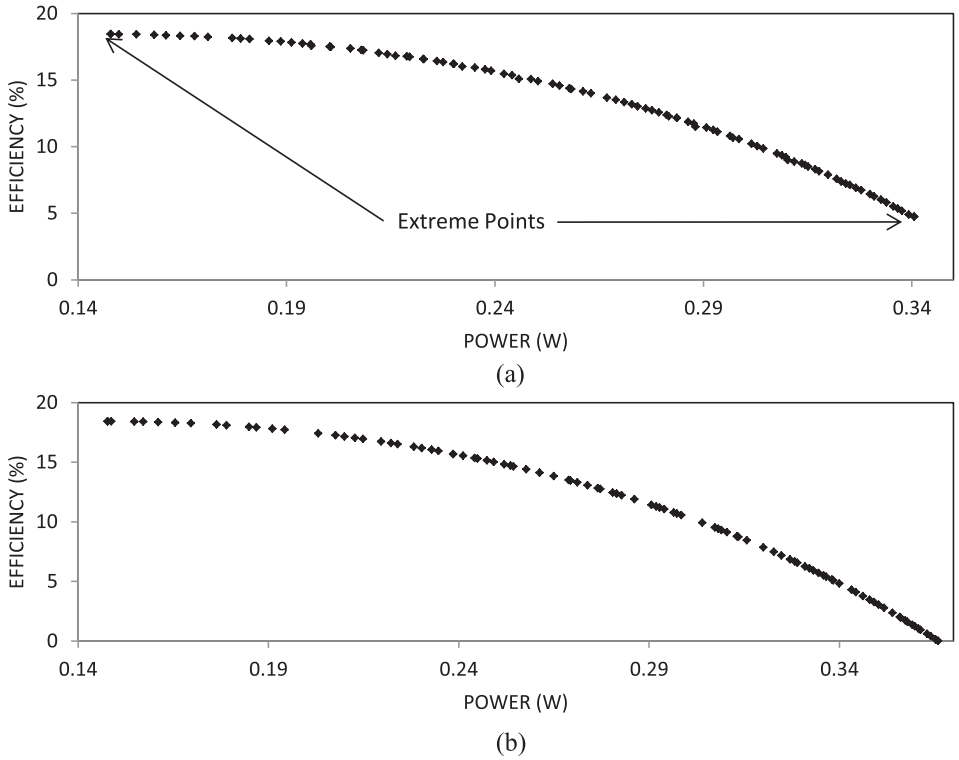

Fig. 3. The best (HV) set of non-dominated solution found by the NSGA-II algorithm. (a) Multi-objective optimization without shape factor. (b) Multi-objective optimization with shape factor.

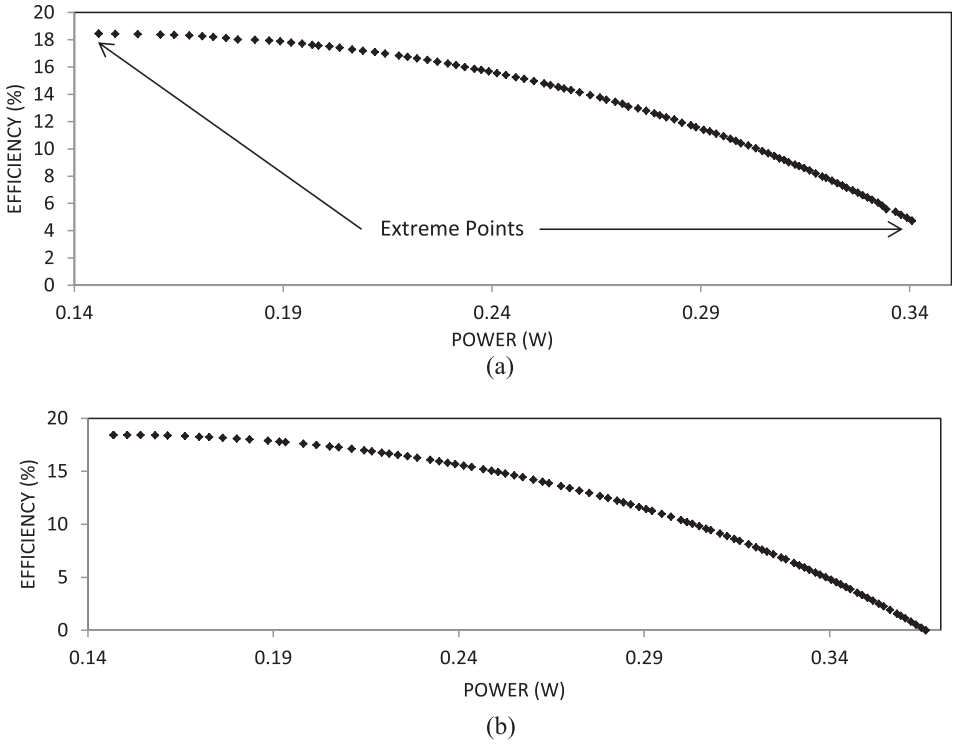

Fig. 4. The best (HV) set of non-dominated solution found by the GDE3 algorithm. (a) Multi-objective optimization without shape factor. (b) Multi-objective optimization with shape factor.

Table 2(a) shows the two extreme (end) solutions obtained through the proposed algorithms. These solutions indicate the maximum possible output power and efficiency that can be achieved through the current design (see Fig. 1(a)) and its variable bounds (see Equations 19–24). The HV results (see Table 3(a)) indicate that the quality of the solutions obtained through these algorithms is comparable. However, GDE3 marginally outperformed the two algorithms in terms of solution accuracy and spread of solutions over

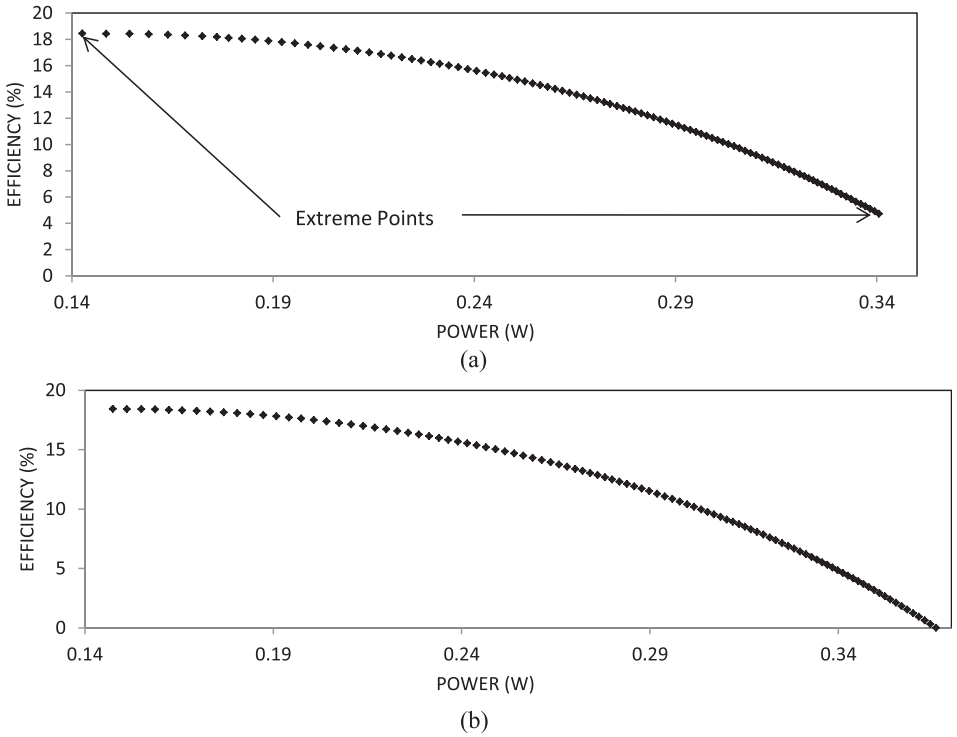

Fig. 5. The best (HV) set of non-dominated solution found by the SMPSO algorithm. (a) Multi-objective optimization without shape factor. (b) Multi-objective optimization with shape factor.

Table 2
The maximum power and efficiency obtained for the optimization problems: a) without the shape factor and b) with the shape factor.

Algorithm	Max. power (Watts)	Max. efficiency (%)
(a)		
NSGA-II	0.3405	18.43
GDE3	0.3393	18.43
SMPSO	0.3405	18.43
(b)		
NSGA-II	0.3659	18.42
GDE3	0.3648	18.42
SMPSO	0.3653	18.42

Table 3
Min, max, mean, and standard deviation of HV measures for the optimization problem: a) without the shape factor and b) with the shape factor.

Algorithm	Min	Max	Mean	St. Dev.
(a)				
NSGA-II	3.752E-03	1.086E-02	9.120E-03	1.665E-03
GDE3	1.002E-02	1.159E-02	1.101E-02	4.203E-04
SMPSO	1.089E-02	3.827E-02	1.209E-02	4.864E-03
(b)				
NSGA-II	2.788E-02	2.824E-02	2.805E-02	7.482E-05
GDE3	2.797E-02	2.818E-02	2.805E-02	3.990E-05
SMPSO	2.799E-02	2.808E-02	2.802E-02	1.935E-05

the Pareto front. Moreover it was able to produce consistent results over many runs, regardless of the initial randomized population.

According to the results found in Ref. [4], at a fixed temperature, the thermoelectric power is a function of the external load resistance. The output power is maximized when $\partial \dot{W}/\partial R_L = 0$. Thus,

$$(R_L)_{\text{opt}} = R \tag{32}$$

$$\dot{W}_{\max} = \frac{\alpha^2 (T_1 - T_2)}{4R} \tag{33}$$

Similarly, a fixed temperature, the thermoelectric efficiency is a function of the external load resistance. The efficiency is maximized when $\partial \eta/\partial R_L = 0$. Thus,

$$(R_L)_{\text{opt}} = R\sqrt{1 + ZT_{\text{avg}}} \tag{34}$$

$$\eta_{\max} = \left. \frac{\alpha^2 (T_1 - T_2) R_L}{K(R_L + R)^2 + \alpha^2 T_1 (R_L + R) - \frac{1}{2}\alpha^2 (T_1 - T_2) R} \right|_{R_L = R\sqrt{1+ZT_{\text{avg}}}} \tag{35}$$

However, the study was only able to obtain the two extreme optimal solutions (i.e., the maximum power and efficiency). Meanwhile all proposed algorithms permitted to find a spectrum of optimal thermal operating conditions as well as device parameters, which would be difficult to find using the analytical analysis conducted in Ref. [4]. The maximum power, based on the lower and upper limits of design and operational parameter settings (Equations (19–24)), is 0.34 W and the efficiency corresponding to the maximum power is 4.73%. Similarly the maximum efficiency is 18.44% and the corresponding power to the maximum efficiency is 0.14 W. Equivalently, the proposed algorithms were able to find these extreme solutions with a margin of error equal to ±0.1%.

Moreover, since the obtain solution set through the proposed algorithms include a spectrum of optimal solutions, it is possible to select a compromising solution acceptable by the designer of the thermoelectric device. For example, one such compromising solution found by the NSGA-II algorithm is 0.19 W of power at 17.81% efficiency (3% drop of efficiency but 29% rise of power). Table 4(a) lists ten (out of 100) non-dominated selected solutions and their corresponding design and operation parameters found by the NSGA-II algorithm (again, based on the best HV measure).

Table 4
Ten selected non-dominated solutions from the best (HV) solution and their corresponding design and operation parameters. (a) Multi-objective optimization without shape factor. (b) Multi-objective optimization with shape factor.

(a)

$\dot{W}$(Watts)	η(%)	T_1(K)	T_2(K)	R_L(Ω)	A_p(m^2)	A_n(m^2)	L_p(m)	L_n(m)
0.14781	18.438	600	273	0.1	7.07×10^{-5}	7.75×10^{-5}	2.12×10^{-3}	2.54×10^{-3}
0.17113	18.229	600	273	0.1	8.93×10^{-5}	9.65×10^{-5}	2.27×10^{-3}	2.41×10^{-3}
0.20037	17.499	600	273	0.1	8.77×10^{-5}	1.31×10^{-4}	1.52×10^{-3}	2.80×10^{-3}
0.22279	16.580	600	273	0.1	1.35×10^{-4}	1.66×10^{-4}	1.91×10^{-3}	2.80×10^{-3}
0.24219	15.459	600	273	0.1	1.35×10^{-4}	1.93×10^{-4}	1.72×10^{-3}	2.36×10^{-3}
0.26301	13.999	600	273	0.1	2.11×10^{-4}	2.30×10^{-4}	1.95×10^{-3}	2.40×10^{-3}
0.28170	12.269	600	273	0.1	1.64×10^{-4}	1.85×10^{-4}	1.09×10^{-3}	1.62×10^{-3}
0.29710	10.656	600	273	0.1	3.73×10^{-4}	1.60×10^{-4}	1.95×10^{-3}	1.11×10^{-3}
0.31365	8.723	600	273	0.1	4.04×10^{-4}	4.78×10^{-4}	1.72×10^{-3}	2.16×10^{-3}
0.32654	6.900	600	273	0.1	3.73×10^{-4}	3.07×10^{-4}	1.06×10^{-3}	1.11×10^{-3}
0.34056	4.734	600	273	0.1	5.01×10^{-4}	5.01×10^{-4}	1.00×10^{-3}	1.00×10^{-3}

(b)

$\dot{W}$(Watts)	η(%)	T_1(K)	T_2(K)	S	L(m)	R_L(Ω)	A_0(m^2)
0.14774	18.418	600	273	0.28172	2.12×10^{-3}	0.1	2.98×10^{-4}
0.17643	18.148	600	273	0.12922	2.09×10^{-3}	0.1	1.48×10^{-4}
0.21485	16.947	600	273	0.27599	2.12×10^{-3}	0.1	2.98×10^{-4}
0.24114	15.545	600	273	0.09131	2.37×10^{-3}	0.1	2.08×10^{-4}
0.26498	13.821	600	273	0.28454	2.10×10^{-3}	0.1	3.41×10^{-4}
0.28615	11.886	600	273	0.15057	3.99×10^{-3}	0.1	1.48×10^{-4}
0.30822	9.402	600	273	0.24851	2.19×10^{-3}	0.1	1.47×10^{-4}
0.32827	6.668	600	273	0.29873	2.36×10^{-3}	0.1	1.50×10^{-4}
0.33998	4.829	600	273	0.28406	3.93×10^{-3}	0.1	1.58×10^{-4}
0.35608	1.967	600	273	0.33645	3.96×10^{-3}	0.1	8.35×10^{-5}
0.36592	0.003	600	273	1.00000	4.00×10^{-3}	0.1	1.00×10^{-6}

3.2. Optimization with the shape factor

To investigate the effect of pin geometry in the optimal thermoelectric device output power and efficiency, a new variable, shape factor, is introduced. When the shape factor is 0, the problem is similar to vertically parallel pin configuration as depicted in Fig. 1(a). Figs. 3(b), 4(b) and 5(b) present the distribution of Pareto-optimal solutions (based on the best HV results) obtained by the proposed algorithms. Table 2(b) show the two extreme solutions obtained through the proposed algorithms. These solutions indicate the maximum possible output power and efficiency that can be achieved through the second thermoelectric device design (see Fig. 1(b)) and its variable bounds (see Equations (25)–(29)). The maximum efficiency attained, under these constraints is ~18.42% and the corresponding power is ~0.147 W. Similarly the maximum power is ~0.365 W and the corresponding efficiency is close to 0%. The corresponding shape factor at this maximum power is $S \approx 1$ (pin vertical slope of ~90°). The HV results (see Table 3(b)) indicate the quality (accuracy and spread) of the solutions obtained through these algorithms is comparable. Similarly, the consistency of results obtained through these algorithms was identical over many runs. Table 4(b) lists ten (out of 100 solutions) selected non-dominated solutions and their corresponding design and operation parameters found by the NSGA-II algorithm.

Fig. 6 shows variation of device output power and efficiency with shape factor of the pins (S) for various temperature ratios (θ), pin leg size (L), and external load parameter (L_R) while Fig. 7 shows three dimensional view of power and efficiency variations with these parameters. Device output power increases sharply with increasing shape factor within the range of 0–0.03, which is more pronounced for low temperature ratios. This is also true for thermal efficiency of the device. This behavior is attributed to the pin electrical resistance (Equation (11)), which has a significant effect on the output power (Equation (16)) and efficiency of the device (Equation (12)).

In this case, small increase in slope modifies the electrical resistance of the device while altering efficiency and device output. Moreover, further increase in shape factor reduces efficiency sharply while device output power remains the same. This is associated with the formulation of efficiency and output power of the device, i.e. efficiency is very sensitive to electrical resistance, since it is a non-linear function of electrical resistance of the pins (Equation (11)).

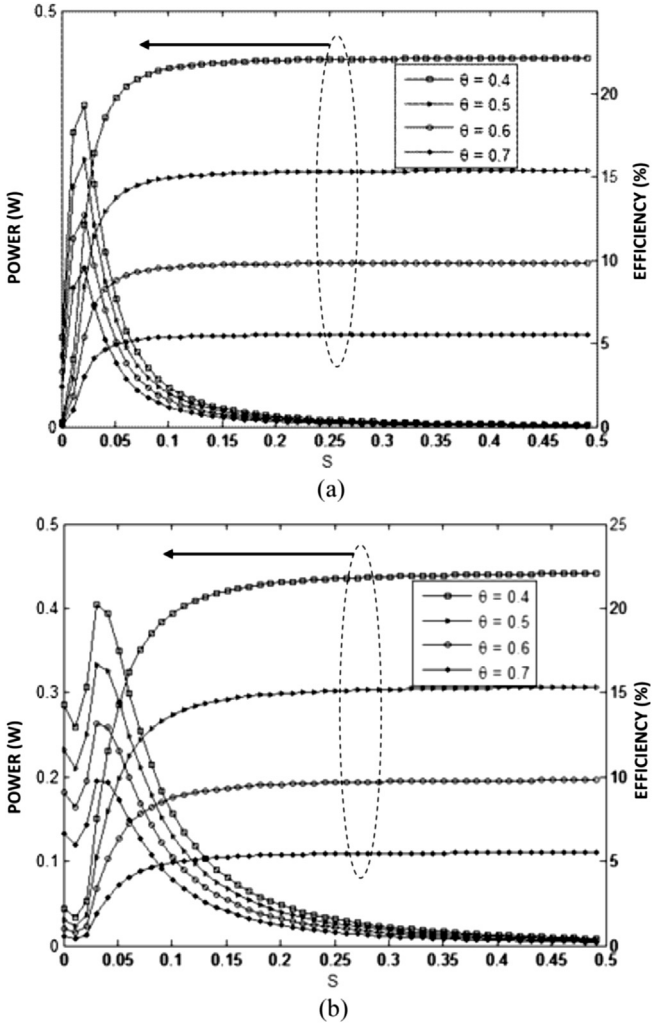

Fig. 6. Variation of thermoelectric power and efficiency with shape factor (S) for different values of temperature ratios: a) pin length $L = 0.004$ m and b) pin length $L = 0.001$ m.

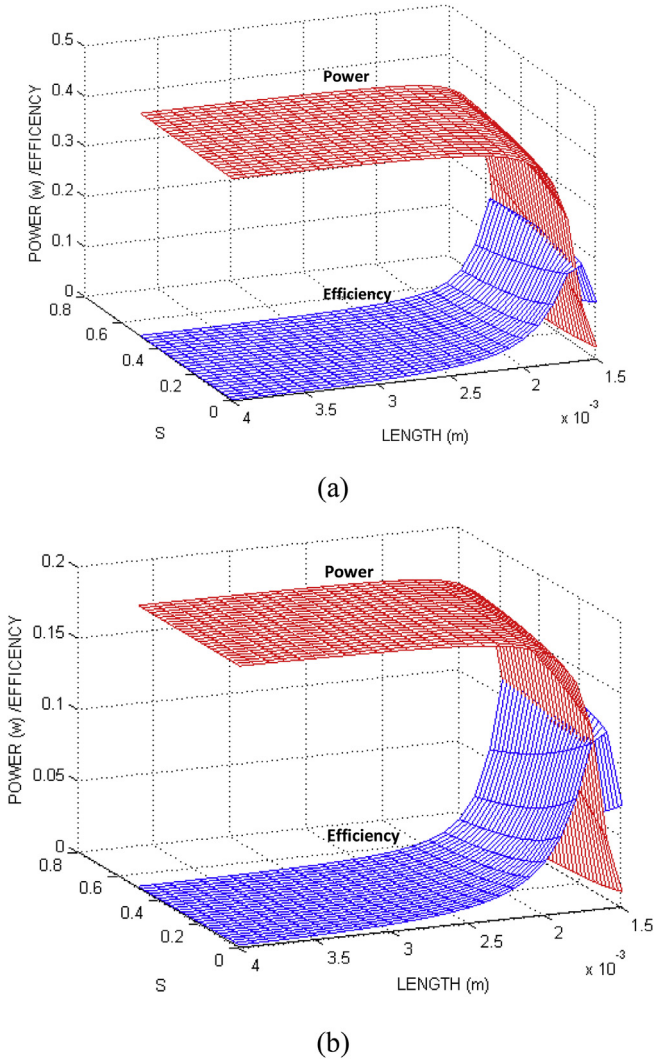

Fig. 7. 3-D view of output power and efficiency with pin length (L) and shape factor (S) for two values of temperature ratio (θ): a) $\theta = 0.4$ and b) $\theta = 0.6$.

Therefore, a small change in electrical resistance causes a large change in efficiency. However, as the shape factor increases further, efficiency remains very low unlike the case observed for the device output. Consequently, device efficiency is sensitive to shape factor up to its critical value; in which case, this behavior changes and the effect of shape factor on device efficiency becomes negligibly small. In the case of device output power, increasing shape factor sharply increases output power, which is true for the value of shape factor less than 0.15. As the value of shape factor increases further device output remains the same. This indicates that the influence of shape factor on efficiency and output power of the device is significant for the values of the shape factor in the range of 0–0.015. Consequently, small deviation of parallel situated pins geometric configuration gives rise to large changes in efficiency and output power of the device. However, as the pin length increases (Fig. 1(b)), the critical value of shape factor influencing efficiency and output power of the device varies. In this case, shape factor attains higher efficiency for longer pin lengths than that corresponding to short pin lengths. This is associated with the electrical resistance of the pins, which increases with the length of the pins. The maximum efficiency and output power of the device does not change considerably with the pin length of the device. Moreover, efficiency and output power of the device increases with increasing temperature ratio. It should be noted that increasing temperature ratio increases the Carnot efficiency of the device; therefore, device efficiency increases accordingly (Equation (12)). This argument is also true for output power of the device (Equation (16)).

Fig. 8 shows variation of efficiency and output power of thermoelectric device with pin length while Fig. 9 shows a three-dimensional (3-D) view of this variation including temperature ratio for two values of the external load parameter (L_R). The pin length for efficiency and output power of the device reaching to their maximum is different, which is more pronounced for shape factor $S = 0.1$. In this case, the pin length corresponding to the maximum efficiency is about 0.15×10^{-3} m while the pin length for the maximum power is in the order of 4×10^{-3} m.

The variation in the pin length for the maximum efficiency and the maximum power is associated with the complex nature of influence of the pin length on efficiency and output power, as given in Equations (12) and (16). However, the efficiency of the device is limited with the pin length in the range of $L \leq 0.75 \times 10^{-3}$ m, which is true for shape factor $S = 0.1$. On the other hand, increasing pin length enhances device output power gradually. Therefore,

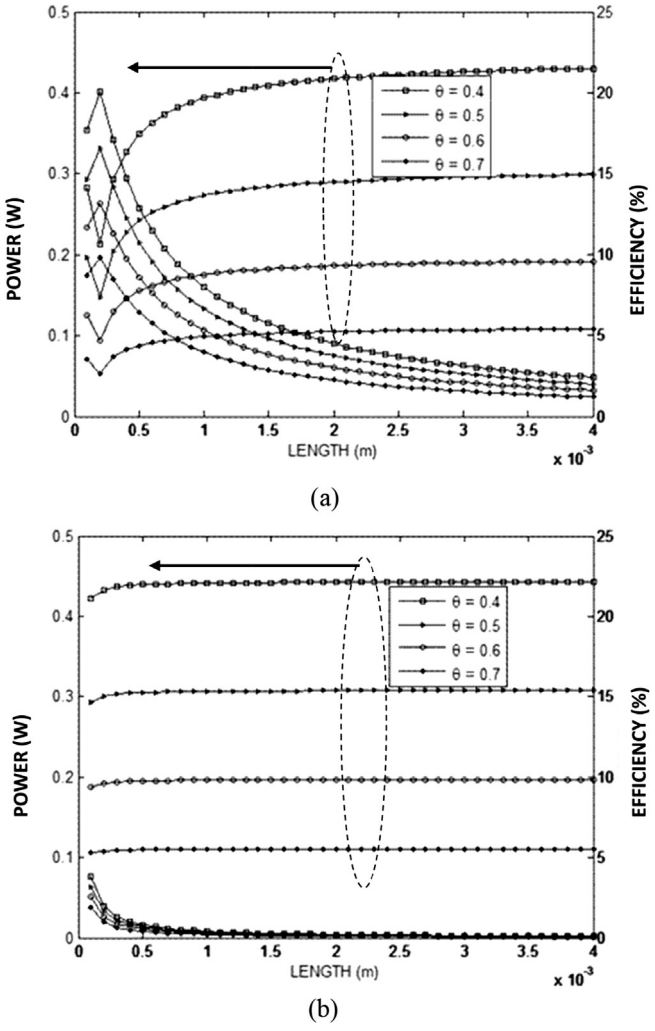

Fig. 8. Variation of thermoelectric power and efficiency with pin length (L) for different values of temperature ratios: a) shape factor $S = 0.1$ and b) shape factor $S = 0.05$.

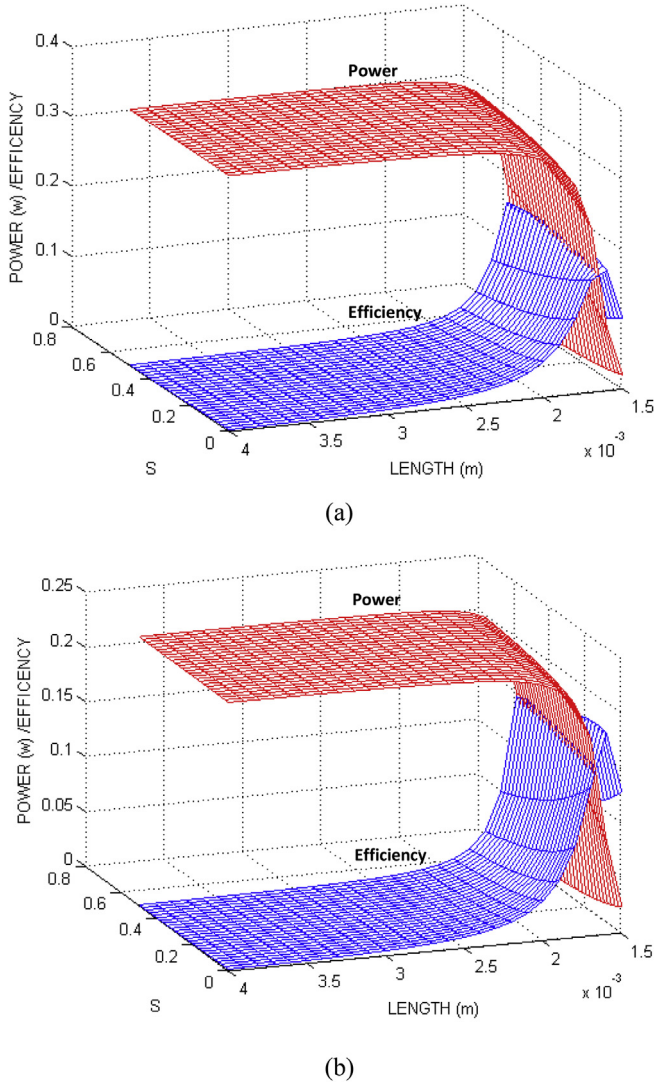

Fig. 9. 3-D view of output power and efficiency with pin length (L) and shape factor (S) for two values of external load parameter (L_R): a) $L_R = 0.1$ and b) $L_R = 0.15$.

variation of pin length is more critical for the attainment of the maximum efficiency than that of the output power.

In the case of shape factor $S = 0.5$, the behavior of both efficiency and output power of the device changes significantly as compared to its counterpart corresponding to shape factor $S = 0.1$. Efficiency remains low for all the values of pin lengths; however, output power remains almost the same with changing pin lengths. This indicates that the effect of pin length on device efficiency and output power is sensitive for small values of shape factor; in which case, coupling effect of shape factor and device pin length on efficiency and output power of the device is significant. Therefore, geometric configuration of thermoelectric device, such as arrangements of vertical slope and length of pins, has a non-linear effect on the device performance characteristics such as efficiency and output power. As shape factor is increased ($S = 0.5$), efficiency and output power of the device becomes almost independent of pin length. Hence, coupling effect of pin shape and pin length on efficiency and output power of the device becomes almost insignificant. Increasing temperature ratio increases efficiency and output power of the device regardless of pin length effect. However, the maximum efficiency reduces significantly for $S = 0.5$ as compared to that of $S = 0.1$, provided that the maximum power remains the same for both of the cases corresponding to $S = 0.1$ and $S = 0.5$.

The geometric configuration based on the shape factor and the pin length does not result in a unique optimum operating condition that maximizes efficiency and output power simultaneously. However, locus of the 3-D plot, where efficiency intersects with output power of the device, indicates the presence of unique geometric configuration of the thermoelectric device, which results in improved efficiency and output power. The points corresponding to the locus of this intersection are given in Tables 5 and 6 for various operational and geometric parameters. The corresponding shape factor and pin length where intersection points take place, changes for different temperature ratios. In addition, the locus of the intersection of efficiency and output power can be considered as the optimum points for designing the device for knowing operating conditions. This is because of the fact that highest output power and efficiency co-exists at locus points of the intersection.

In the case of Table 6, increasing temperature ratio (θ) lowers output power and efficiency at locus points of the intersection. The highest efficiency and output power are possible for a temperature ratio of 0.4. Consequently, increasing temperature ratio increases thermal efficiency (Fig. 6); however, this increase does not yield the highest possible output power at the point of the maximum efficiency. Similarly, increasing temperature ratio enhances output power (Fig. 6); however, efficiency becomes low when output power is high. In the case of the optimum external load parameter (R_L), as given in Table 6, $R_L = 1$ results in highest efficiency and highest output power. However, further increase or reduction in R_L, device efficiency and output power are reduced simultaneously. Consequently, the optimum design configuration is present for a unique value of external load parameter.

Table 5
Points at the locus of intersection of efficiency and output power of the device for different values of temperature ratios (θ).

Shape factor (S)	Length (L)	Power (W)	Efficiency (η)
$\theta = 0.4$			
0.500	0.00102	0.2001	0.2001
0.419	0.00159	0.2017	0.2017
0.293	0.00161	0.2021	0.2021
0.067	0.00163	0.2029	0.2029
$\theta = 0.5$			
0.500	0.00160	0.1604	0.1604
0.401	0.00160	0.1562	0.1562
0.227	0.00162	0.1614	0.1614
0.99	0.00164	0.1614	0.1614
$\theta = 0.6$			
0.500	0.00160	0.1222	0.1222
0.409	0.00162	0.1202	0.1202
0.333	0.00164	0.1206	0.1206
0.067	0.00167	0.1203	0.1203
$\theta = 0.7$			
0.499	0.00164	0.0791	0.0791
0.381	0.00165	0.0781	0.0781
0.235	0.00167	0.0783	0.0783
0.093	0.00170	0.0784	0.0784

Table 6
Points at the locus of intersection of efficiency and output power of the device for different values of external load parameter (R_L).

Slope (S)	Length (L)	Power (W)	Efficiency (η)
$R_L = 0.05$			
0.499	0.00158	0.1692	0.1692
0.349	0.00159	0.1696	0.1696
0149	0.00161	0.1697	0.1697
0.029	0.00163	0.1695	0.1695
$R_L = 0.1$			
0.491	0.00159	0.1771	0.1771
0.369	0.00160	0.1804	0.1804
0.179	0.00162	0.1805	0.1805
0.015	0.00165	0.1807	0.1807
$R_L = 0.15$			
0.499	0.00160	0.1502	0.1502
0.349	0.00161	0.1583	0.1583
0.175	0.00163	0.1581	0.1581
0.019	0.00166	0.1575	0.1575

3.3. Modeling locus points of intersection

As discussed in the previous section, the locus of the intersection of efficiency and output power can be considered as the optimum points for designing the device for knowing operating conditions. This is because of the fact that highest output power and efficiency co-exists at locus points of the intersection. Therefore we are interested in the mathematical formula that describes the relationship between thermal efficiency (η) and load resistance (R_L), shape factor (S) and pin length (L) as well as output power ($\dot{W}$) and temperature ratio (θ), shape factor (S) and pin length (L) using experimental data collected from the optimization step (see Tables 4 and 6). Genetic Programming (i.e. symbolic regression based on evolutionary computation) is used to establish the mathematical expression while minimizing the error metrics. Genetic programming is an evolutionary approach, in which programs/symbols (nonlinear representation based on trees) evolved to solve a given task [28].

Using genetic programming based application [29] (with 1.08×10^{-8} mean squared error) the thermal efficiency as a function of external load resistance (R_L), shape factor (S) and pin length (L) at locus points of intersection can be written as:

$$\eta(R_L, S, L) = 0.1257 + 1.231R_L + 0.9348S + 0.2859R_LS - 6.786R_L^2 - 593SL - 1.17R_LS^3.$$

Similarly, using genetic programming (with 1.33×10^{-6} mean squared error) the thermal output power as a function of temperature ratio (θ), shape factor (S) and pin length (L) at locus points of intersection can be written as:

$$\dot{W}(\theta, S, L) = -0.1039 + 295.2L + 0.03667S + 1.153S^2 + 0.1822\theta S^2 - 270.3\theta L - 802.7S^2L.$$

In general, it is recommended that for a fixed operational condition including external load parameter and temperature ratio, non-parallel pins are favorable with the shape factor (S) within the range $0.2 \leq S \leq 0.5$ because of achieving high efficiency and output power of the device. In the case of the operating conditions, decreasing temperature ratio ($\theta \approx 0.4$) enhances device efficiency and output power when the optimum design conditions are satisfied.

4. Conclusion

Thermal analysis of thermoelectric generator is considered and influence of geometric features on efficiency and output power of the device is examined. A multi-objective optimization study is carried out to maximize the efficiency and output power of a thermoelectric device including the geometric features of shape factor and pin length, as well as operational parameters such as temperature ratio and external load parameter. The utilized multi-objective algorithms (NSGA-II, GDE3, and SMPSO) enabled to find a diverse set of optimal solutions which would be difficult to find using analytical methods. For example, some intermediate solutions could be of interest with regards to other non-expressed objectives or secondary objectives such as operating conditions, device dimension or other technical aspects. Overall the performance of the three algorithms was comparable. However, GDE3 marginally outperformed the two algorithms in terms of solution accuracy and spread of solutions over the Pareto front. Moreover, GDE3 was able to produce slightly better consistent results over many runs.

It is found that small change in shape factor alters thermal efficiency and output power. In this case, efficiency, first, increases to reach its maximum and, later, reduces sharply with increasing shape factor. Output power also increases sharply and remains the same with increasing shape factor. The similar effect is also observed for the size of pin length. In any case, the geometric feature of the device corresponding to the maximum efficiency does not give rise to the maximum output power. This is associated with the complex effect of shape factor and pin length on the device efficiency. Thermal efficiency reduces significantly for large value of shape factor ($S = 0.5$), which corresponds to 45° vertical slope of pins. In addition, output power remains almost the same for varying pin length size for $S = 0.5$. This indicates that output power of the thermoelectric device maintains high regardless of pin length size, provided that thermal efficiency reduces significantly. The locus of the intersection of efficiency and output power, due to different geometric configurations, can provide the optimum design configurations of the thermoelectric device; in which case, a unique geometric configuration is resulted for the fixed operating conditions. Increasing temperature ratio or external load parameter alters the geometric configuration corresponding to the optimum efficiency and output power of the device. Therefore, for a fixed operational condition, non-parallel pins are favorable because of achieving high efficiency and output power of the device. In addition, decreasing temperature ratio enhances device efficiency and output power when the optimum design conditions are satisfied.

Acknowledgments

The authors acknowledge the support of the University of Ontario Institute of Technology (NSERC Discovery Grant) and the Thermoelectric Group at King Fahd University of Petroleum and Minerals, Dhahran, Saudi Arabia for this work.

Nomenclature

A_o	average (mid-height) cross-sectional area
I	electrical current
K	thermal conductance of the thermoelectric generator
K_0	the reference thermal conductance
$K_{e,p}$	p-type electrical conductivity
$K_{e,n}$	n-type electrical conductivity
K_{leg}	overall thermal conductance of the pin
K_n	n-type thermal conductivity
K_p	p-type thermal conductivities
L	height of the pin
L_R	external load parameter
$\dot{Q}$	the rate of heat transfer along the x-axis in the pin
R	overall electrical resistivity of the thermoelectric generator
R_0	the reference electrical resistivity
r_k	thermal conductivity ratio
r_{ke}	electrical conductivity ratio
R_L	external load resistance
R_{leg}	overall electrical resistance of the pin
S	shape factor of the pin
T_{ave}	average temperature
T_1 or T_R or T_H	hot side temperature of the thermoelectric generator
T_2 or T_L	cold side temperature of the thermoelectric generator
$\dot{W}$	electrical power output from the thermoelectric generator
Z	figure of merit $= \alpha^2/KR$
α	the difference between the Seebeck coefficients of p and n junctions
α_n	n-junction Seebeck coefficient
α_p	p-junction Seebeck coefficient
δ	the thickness of the pin
θ	temperature ratio $= T_2/T_1$
η	efficiency of the thermoelectric generator
μ	dimensionless slope parameter

References

[1] Vining C. An inconvenient truth about thermoelectrics. Nat Mater 2009;8:83–5.
[2] Sahin AZ, Yilbas BS. Thermodynamic irreversibility and performance characteristics of thermoelectric power generator. Energy 2013;55:899–904.
[3] Sahin AZ, Yilbas BS. The thermoelement as thermoelectric power generator: effect of leg geometry on the efficiency and power generation. Energy Convers Manag 2013;65:26–32.
[4] Sahin AZ, Yilbas BS. The influence of operating and device parameters on the maximum efficiency and the maximum output power of thermoelectric generator. Int J Energy Res 2012;36:111–9.
[5] Wang CC, Hung CI. Effect of irreversibilities on the performance of thermoelectric generator investigated using exergy analysis. J Therm Sci Technol 2013;8(1):1–14.
[6] He W, Su Y, Riffat SB, Hou J, Ji J. Parametrical analysis of the design and performance of a solar heat pipe thermoelectric generator unit. Appl Energy 2011;88(12):5083–9.
[7] Patyk A. Thermoelectric generators for efficiency improvement of power generation by motor generators - environmental and economic perspectives. Appl Energy 2013;102:1448–57.
[8] Shu G, Zhao J, Tian H, Liang X, Wei H. Parametric and exergetic analysis of waste heat recovery system based on thermoelectric generator and organic Rankine cycle utilizing R123 source. Energy 2012;45(1):806–16.
[9] Wee D. Analysis of thermoelectric energy conversion efficiency with linear and nonlinear temperature dependence in material properties. Energy Convers Manag 2011;52(12):3383–90.
[10] Kim S. Analysis and modeling of effective temperature differences and electrical parameters of thermoelectric generators. Appl Energy 2013;102:1458–63.
[11] Chen M, Lund H, Rosendahl L, Condra TJ. Energy efficiency analysis and impact evaluation of the application of thermoelectric power cycle to today's CHP systems. Appl Energy 2010;87(4):1231–8.

[12] Rao V, Patel V. Multi-objective optimization of two stage thermoelectric cooler using a modified teaching–learning-based optimization algorithm. Eng Appl Artif Intell 2013:430–45.
[13] Belanger S, Gosselin L. Multi-objective genetic algorithm optimization of thermoelectric heat exchanger for waste heat recovery. Int J Energy Res 2012: 632–42.
[14] Wang J, Yan Z, Wang M, Dai Y. Thermodynamic analysis and optimization of an ammonia-water power system with LNG (liquefied natural gas) as its heat sink. Energy 2013;50(1):513–22.
[15] Hajabdollahi Z, Hajabdollahi F, Tehrani M, Hajabdollahi H. Thermo-economic environmental optimization of Organic Rankine Cycle for diesel waste heat recovery. Energy 2013;63:142–51.
[16] Sayyaadi H, Aminian HR. Design and optimization of a non-TEMA type tubular recuperative heat exchanger used in a regenerative gas turbine cycle. Energy 2010;35(4):1647–57.
[17] Daroczy L, Janiga G, Thevenin D. Systematic analysis of the heat exchanger arrangement problem using multi-objective genetic optimization. Energy 2014;65:364–73.
[18] Ibrahim A, Bourennani F, Rahnamayan S. Optimal photovoltaic farm design using multi-objective optimization. Int J Appl Metaheuristic Comput (IJAMC) 2013;4(4):63–89.
[19] Saraswat A, Saini A, Saxena AK. A novel multi-zone reactive power market settlement model: a pareto-optimization approach. Energy 2013;51: 85–100.
[20] Li Y, Jia M, Chang Y, Liu Y, Xie M, Wang T, Zhou L. Parametric study and optimization of a RCCI (reactivity controlled compression ignition) engine fueled with methanol and diesel. Energy 2014;65:319–32.
[21] Ippolito MG, Di Silvestre ML, Sanseverino RR, Zizzo G, Graditi G. Multi-objective optimized management of electrical energy storage systems in an islanded network with renewable energy sources under different design scenarios. Energy 2014;64:648–62.
[22] Ahmadi P, Dincer I, Rosen MA. Thermoeconomic multi-objective optimization of a novel biomass-based integrated energy system. Energy 2014;68:958–70.
[23] Liu N, Chen Z, Liu J, Tang X, Xiao X, Zhang J. Multi-objective optimization for component capacity of the photovoltaic-based battery switch stations: towards benefits of economy and environment. Energy 2014;64: 779–92.
[24] Shi X, Yang J, Salvador JR, Chi M, Cho JY, Wang H, Bai S, Yang J, Zhang W, Chen L. multiple-filled Skutterudites: high thermoelectric figure of merit through separately optimizing electrical and thermal transports. J Am Chem Soc 2011;133(20):7837–46.
[25] Talbi E. Metaheuristics from design to implementation. John Wiley & Sons Publication Inc; 2009. p. 308–20.
[26] Deb K, Pratap A, Agarwal S, Meyarivan T. A fast and elitist multiobjective genetic algorithm: NSGA-II. Evol Comput IEEE Trans 2002;6(2):182–97.
[27] Zitzler E, Thiele L. Multiobjective evolutionary algorithms: a comparative case study and the strength Pareto approach. Evol Comput IEEE Trans 1999;3(4): 257–71.
[28] Koza JR. Genetic programming. Cambridge, MA: MIT Press; 1992.
[29] Schmidt M, Hod L. Distilling free-form natural laws from experimental data. Science 2009:81–5.
[30] Nebro AJ, Durillo JJ, Garcia-Nieto J, Coello Coello CA, Luna F, Alba E. SMPSO: a new PSO-based metaheuristic for multi-objective optimization. In: Computational intelligence in multi-criteria decision-making, mcdm'09. IEEE symposium; 2009. p. 66–73.
[31] Kukkonen S, Lampinen J. Performance assessment of generalized differential evolution 3 (GDE3) with a given set of problems. In: Proceedings of the IEEE Congress on evolutionary computation; 2007.
[32] Tan KC. CEC 2007 conference report. IEEE Comput Intell Mag 2008;3:72–3.
[33] Kukkonen S, Lampinen J. GDE3: the third evolution step of generalized differential evolution, evolutionary computation. In: 2005 IEEE Congress on Evolutionary Computation, vol. 1; 2005. p. 443–50.
[34] Kennedy J, Eberhart RC. Particle swarm optimization. In: Proceedings of the 1995 IEEE International Conference on Neural Network, Vol. 4. IEEE Press; 1995. p. 1942–8.
[35] Silva JC, Cruz G, Vinhal C, Silva DR, Bastos-Filho CJ. Comparing MOPSO approaches for hydrothermal systems operation planning. In: Computational Intelligence and 11th Brazilian Congress on Computational Intelligence (BRICS-CCI & CBIC); 2013. p. 551–6.